# Classification of Radial Wind Profiles for Gulf of Mexico Tropical Cyclones

Andrew T. Cox
*Oceanweather Inc.*
*Cos Cob, CT, USA*

## 1. INTRODUCTION

Traditional deductive approaches based on a single vortex representation of a tropical cyclone applied in joint probability method studies have relied on the imposition of correlations between intensity and radius and/or intensity and Holland's B, leaving fewer variables to randomize. No such correlations exist for the double vortex model, which is applied in cases where tropical surface radial wind profiles depict a double wind maxima or "shelf-like" structure to the radial wind profile beyond the primary radius of maximum winds. The shape of the radial wind profile in a tropical cyclone has been shown to have a significant impact on the ocean response (Cardone and Cox, 2009).

This study applies a database of single and double exponential pressure profile fits developed for ocean response modeling in the Gulf of Mexico (GOM) to build a new classification system based on the radial wind profile of tropical cyclones. A "shelf" index is developed to aid in a seven class profile classification system which is applied to 4,043 profile fits in 396 Gulf of Mexico tropical cyclones from the period 1900-2011. Relationships of each profile class are explored as well as dependencies on track history, time of year, intensity and forward speed.

## 2. TROPICAL RADIAL WIND PROFILE CLASSIFICATION

### 2.1 Previous Work

It has been long recognized that hurricanes and tropical cyclones in other basins exhibit a wide variety of sizes. Colon (1963) studied aircraft reconnaissance flight level measured radial wind profiles of various North Atlantic Basin storms and introduced a two-class description. A given cyclone resembled either Hurricane Daisy (1958) with a small eye diameter and extent of wind circulation or Hurricane Helene (1958) of relatively large eye diameter and wind field extent. Notable examples of the Daisy and Helene types studied included GOM Hurricane Carla (1961), a Helene type, and Hurricane Ione (1955). Colon expressed size in terms of the rate of decay of the flight level wind speed with respect to radius. For example, in one Daisy profile, with the storm at minimum central pressure (Po) of 950 mb, the wind speed decayed from a peak of 115 knots at its radius of maximum wind speed of 10 nautical miles (Nm) to 35 knots at a radius of 60 Nm. In Helene, on the other hand, while it was at intensity 942 mb, the peak wind speed of 105 knots at a radius of 15 Nm decayed only to 70 knots at a radius of 60 Nm. Colon found the Helene type to be more common than the Daisy type. Also, storms of the Helene type that intensified tended to contract toward the Daisy type, while no such correlation of intensity changes was found with changes in the Daisy type wind profile.

Merrill (1984) looked at the variability of size of tropical cyclones in both the North Atlantic and North Pacific Basins but used simply the radius of the outer closed isobar as a "size index". He found that western Pacific typhoons average larger sizes than Atlantic hurricanes, explored seasonal variability in size (in both basins sizes trended larger in October), and suggested the role of size in angular momentum losses. This latter observation was much later expanded in a theory (see below) that proposed that tropical cyclones of the most extreme intensity must be small. Merrill found that intensity changes were very weakly correlated with size changes.

Samsury and Rappaport (1991) expanded the types of radial wind profiles commonly exhibited by flight level radial profiles of tangential wind speed to the five types in their paper as shown here in Figure 1.

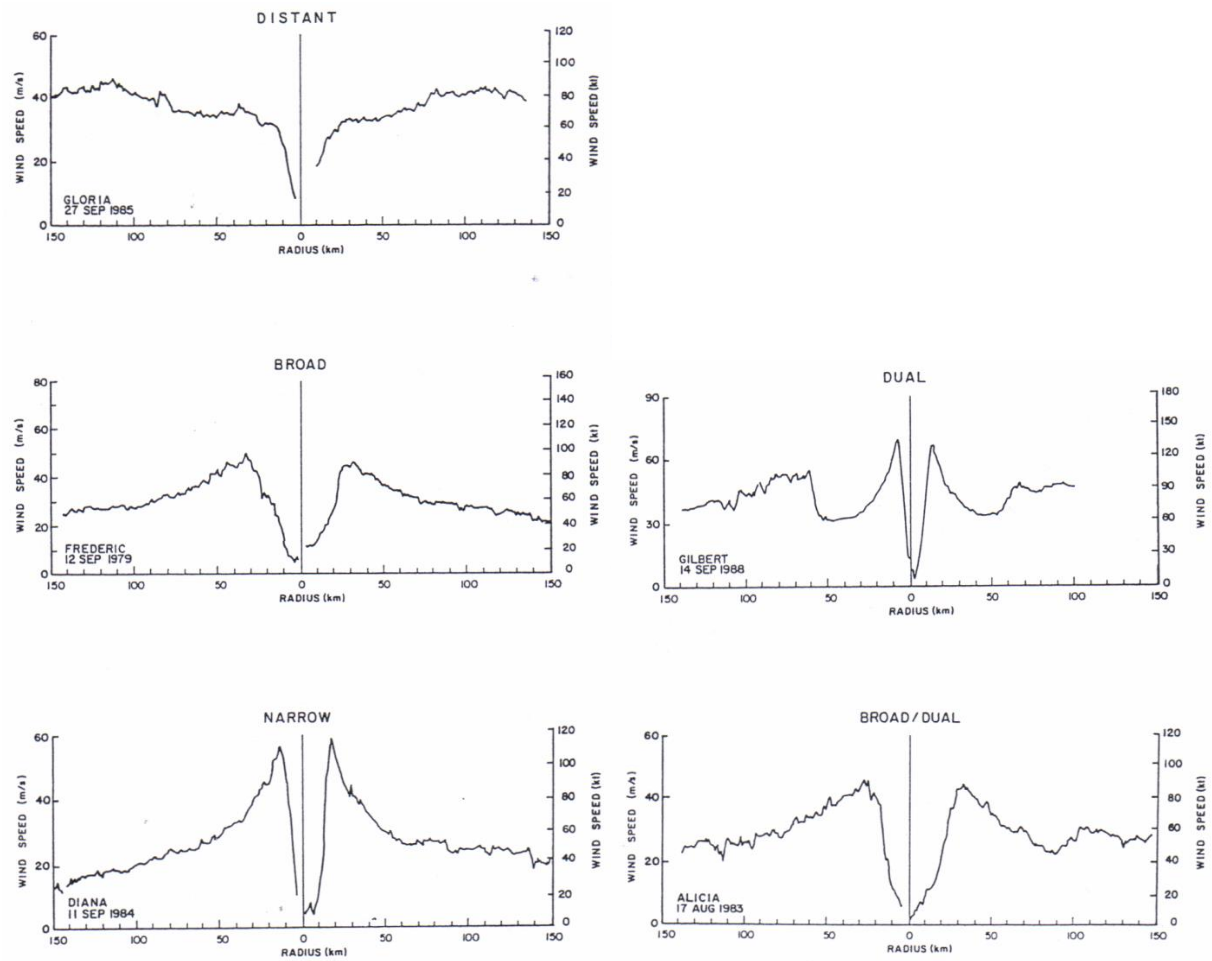


**Figure 1. Sample radial wind profiles reproduced from Samsury and Rappaport (1991)**

Their "Narrow" class is akin to Colon's Daisy-type and their "Broad" class to Colon's Helene-type. Note that their "Distant" category indicates a radial wind profile with no distinct wind speed maxima, suggestive of a shelf like profile. These were found to be usually associated with Category 1 or 2 hurricanes. Narrow storms were usually associated with Category 3-5 hurricanes. Intensity changes were explored and it was suggested that changes of the order of 10-15 knots could be predicted if related to characteristic changes in the profile from one class to another.

Chen et al. (2010) studied size variability of tropical cyclones by analyzing surface wind distributions in 171 western North Pacific typhoons between 2000-2007 that were well monitored by the QuikSCAT scatterometer. Cyclone states were classified as "compact" or "incompact" based on a dimensionless structure parameter, S, defined as:

$$S = \frac{Vt_{2RMW}RMW}{(Vt_{2RMW}RMW)_{ave}}$$

where $Vt_{2RMW}$ is the tangential wind speed at twice the radius of maximum wind, and the denominator is the average value of the product over the total storm sample studied. This formulation imparts a characteristic size based on both the relative RMW and the rate of decay of the wind speed from RMW to twice RMW. A value of $S < 1$ is more "compact" than average and $S > 1$ is less compact (hence, "incompact") than average. More clearly defined cases were delineated at S thresholds at the 33rd and 67th percentiles of the overall distribution of S. Chen et al. attempt to relate S to intensity and intensity changes and found that a compact structure is conducive to intensification with mean intensification rates of about 10 m/s in 24-hours. Compact cyclones are also more likely to approach their maximum potential intensity (MPI) while incompact cyclones tend to fill (weaken). Figure 2, from Chen et al. shows typical structures of compact and incompact typhoons.

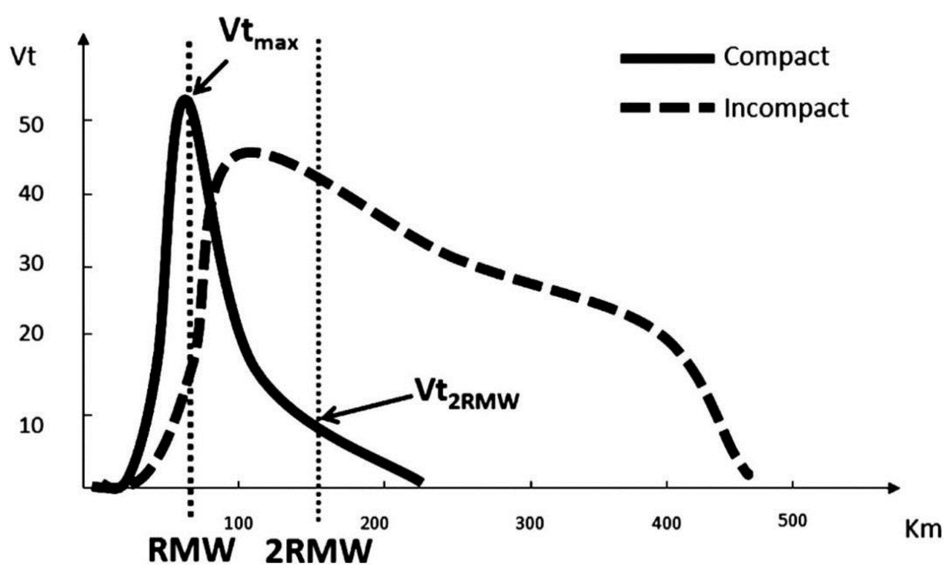


**Figure 2. Schematic showing the definition of Vtmax, Vt2RMW, RMW, and 2RMW. Typical structures of a compact TC (solid line) and an incompact TC (dashed line) are shown (from Chen et al. 2010).**

It is interesting to note that all of the above studies have attempted to relate cyclone size and changes in size to intensity changes. It is well known that real time forecasting of cyclone intensity changes remains a daunting problem despite considerable attempts to apply statistical, as well as dynamical, ensemble and super-ensemble approaches. Therefore, the indications of the above studies appear to provide merely another part of the forecaster's intensity prediction toolbox.

The issue of the relationship of size to intensity is just as critical for the specification of the climatological characteristics of a population of synthetic storms from which ocean response criteria are intended to be developed. At very long recurrence intervals, it is crucial to specify the size and structure of hurricanes that are approaching their MPI. This question was explored by Shen (2006) in terms of the kinetic energy balance within a hurricane. It was found that small size hurricanes tend to develop into more intense hurricanes since surface dissipation of kinetic energy is confined to a small area of high winds and is, therefore, more constrained that hurricanes with large circulations, relative to kinetic energy generation by local surface entropy flux, which is less sensitive to size. Figure 3, from Shen (2006), indicates that this conclusion is fairly robust on the assumption of the exchange coefficients for heat and momentum used in the balance energy budget calculation.

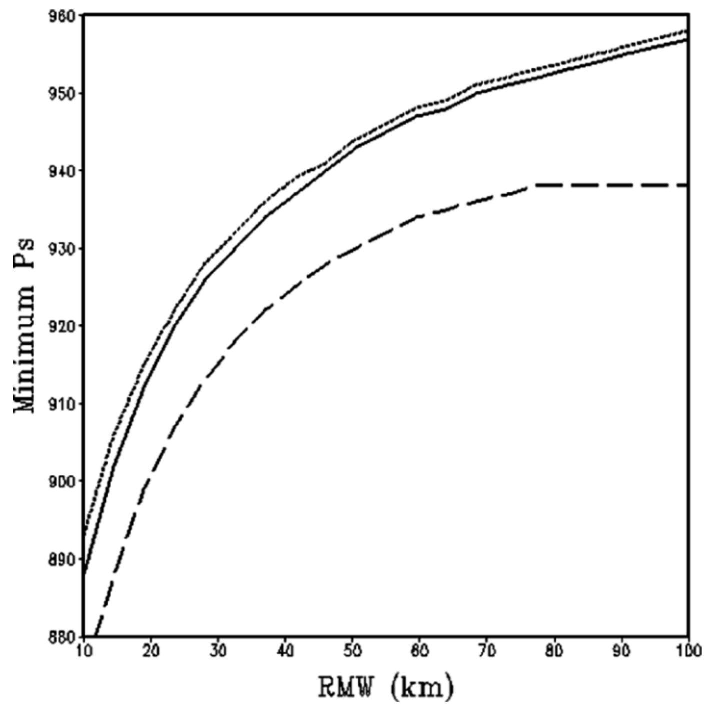


**Figure 3. Potential intensity as a function of RMW with different drag (Cd) and heat exchange (Ch) coefficients under high wind conditions (>35 m/s). Solid: with constant Cd and Ch under high winds. Dotted: with Cd and Ch under high winds extrapolated based on the linear wind-exchange coefficient relations attained in low-to-moderate wind regimes. Dashed: different from the dotted with only Cd leveling off under high winds (from Shen 2006).**

While Shen's model is conceptually appealing, several recent GOM hurricanes that have approached their MPI (in terms of minimum central pressure) appear not to conform to a simple direct size-intensity relationship, particularly after they are examined in terms of the profile analyses presented in this study. For example, Figure 4 shows the azimuthal mean radial wind profile of Hurricane Allen (1980) at Po of 909 mb. Indeed, the inner RMW is very small at ~ 7 Nm, but there is broad circulation with a distinct second RMW at ~ 70 Nm. Hurricane Opal (1995) at Po of 915 mb contained a small inner eye with RMW ~7 Nm, but the circulation exhibits also a broad shelf of hurricane wind speeds in the radius range of 30 Nm to 60 Nm. Hurricane Katrina (2005) is perhaps the most egregious exception. When its Po was in the Category 5 range of 902 mb to 915 mb, its RMW was generally in the range 15 Nm to 20 Nm and increased to as large as ~30 Nm before significant filling commenced. Hurricane Camille (1969) at 902 mb with RMW in the 5 – 10 Nm range is perhaps the quintessential manifestation of Shen's model but there was little reconnaissance data to allow a detailed study of its radial wind speed profile. Hurricane Rita (2005) at 897 mb is a good example of a well-documented small hurricane approaching its MPI and of small size though this hurricane later expanded to become a large intense storm. These examples suggest that a simple two-class system such as Colon's "Daisy and Helene" types or Chen et al.'s "Compact and Incompact" classes are too simple to encompass the range of variability exhibited by major GOM hurricanes.

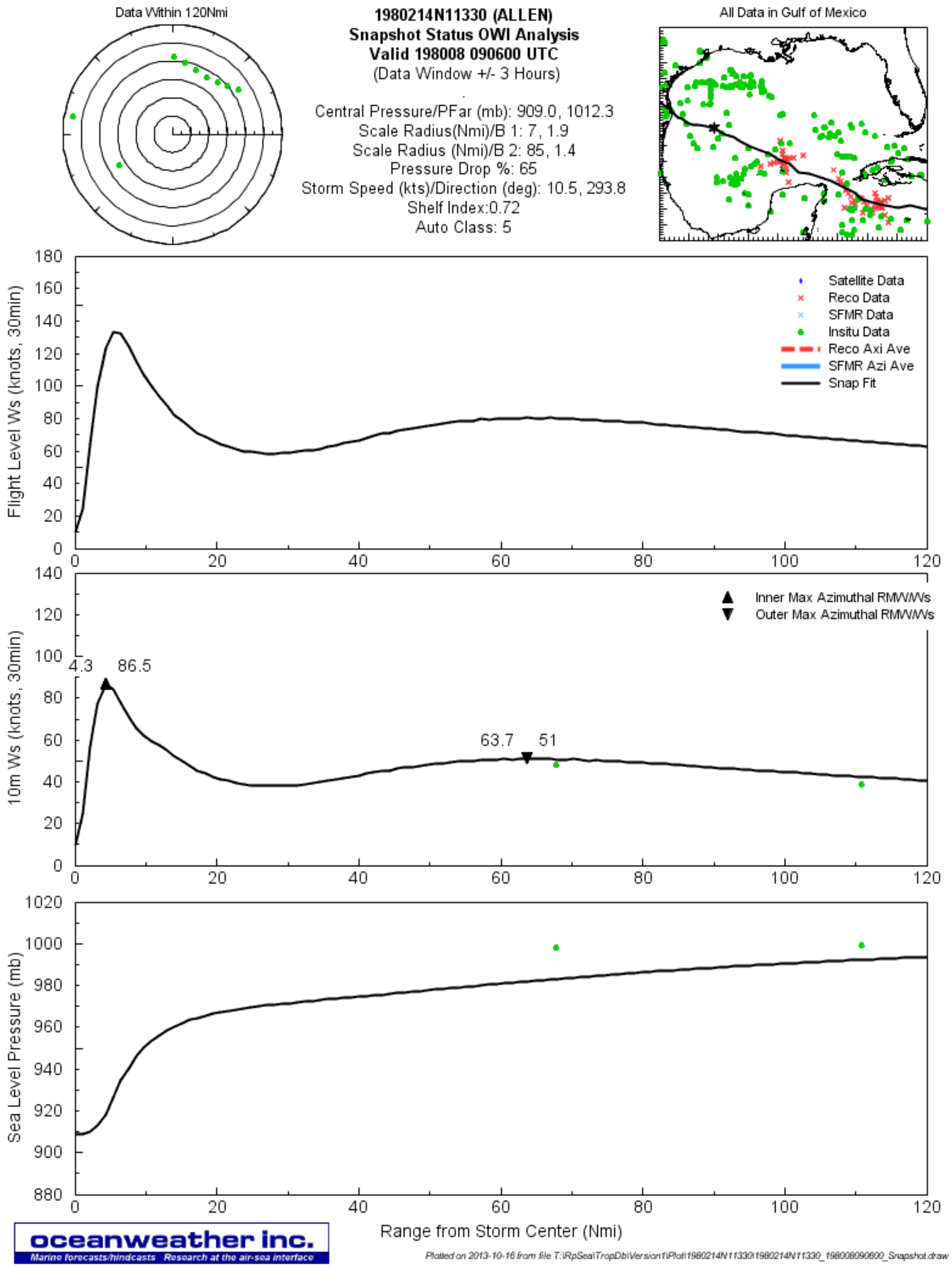


**Figure 4. Summary of available data with profile fits to Allen (1980) valid Aug-09-1980 06:00 UTC**

## 2.2 Gulf of Mexico Oceanographic Study (GOMOS)

In order to build a new classification for radial wind profile fits, a database of such fits was required. The GOMOS2008 hindcast modeled all tropical systems in the GOM from 1900-2008, thus a ready database of tropical fits was available for analysis. At the time of this climatology, years 2009-2011 were available for inclusion as well as the original GOMOS 1900-2008 period.

A search of the GOMOS fit database from 1900-2011 yielded 4,043 individual fits in 396 storms which entered the region depicted in Figure 5. Snapshots are typically derived every 6 hours during the storm lifetime, with sub-six hour snapshot specified at landfall or during times of rapid change and/or track deviation from an interpolated 6-hourly path.

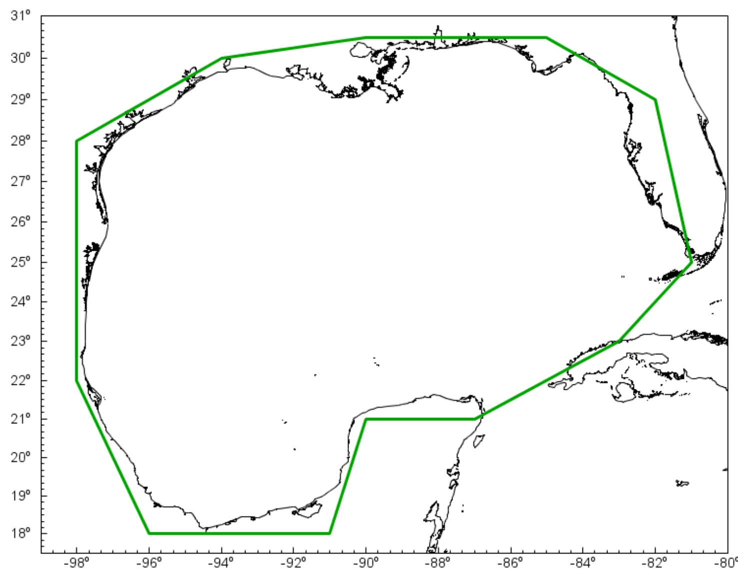


**Figure 5. Search domain for GOM tropical snapshot parameters**

## 2.3 Diagnostic Plots for Assignment of Classes to GOMOS Snapshots

The first step in the assignment of classes to each GOMOS snapshot was to produce a packet of diagnostic plots of each snapshot fitted by storm. Figure 6 gives a sample overall summary for Rita (2005), a Category 5 storm that entered the GOM through the Florida Straits and made landfall near the Texas-Louisiana border. The summary plot in the packet displays the time history of the snap-fit parameters which include central pressure, far field pressure, Rad 1 and Rad 2, Holland's

B1 and B2 and the percentage of the pressure drop (Dp%) carried by the first exponential. Each individual snapshot time is summarized in plots like Figure 4 which shows all available measured wind and pressure data available for each individual fit plotted as a function of distance from the center. The data are typically a 3-hour composite centered on the snap-fit time shown and are displayed within 120 Nm of the center. The data include remotely sensed wind speeds, reconnaissance flight level winds (reduced to the 10 m), the Step Frequency Microwave Radiometer (SFMR) along individual flight legs as well as their azimuthal averages, the snap-fit azimuthal average flight level wind speed, the modeled 10-m level wind speed (30-minute average) compared as well to insitu data from ships, buoys, C-Man stations and coastal stations for equivalent marine exposure, and the surface radial sea level pressure profile, also with in-situ data shown for comparison.

The amount of insitu, satellite and aircraft data varies from storm to storm and from time step to time step. The diagnostic snapshots were used to rate the data availability in seven classes (DC0 through DC6) as depicted in Figure 7 which range from no data (DC0) to high resolution data in all quadrants (DC6). The overall distribution (Figure 8) of snapshots by data class show the majority of the snapshots are either DC0 (no data, 31% of the snapshots) or DC1 (insitu/satellite incomplete, 34% of the snapshots). The data classes which represent data in all quadrants (DC2, DC4 and DC6) make up just 20% of the total population. Fitting of the double exponential pressure profile option in the model is applied in more complex radial wind profiles, so it is not surprising that most (73%) double exponential fits are applied when high resolution aircraft reconnaissance (DC5 and DC6) are available (Figure 9). When the data classes are stratified by year (Figure 10), several interesting patterns emerge. Most data void snapshots (DC0) are in the period previous to 1950. "Sparse" reconnaissance (DC3 and DC4) began in the late 1940's and continue primarily until high-resolution aircraft data (DC 5 and DC6) become available in 1989. "Sparse" aircraft data have nearly 3.2 times more incomplete than good coverage while high-resolution aircraft classes have roughly equal numbers of incomplete and good coverage in all quadrants.

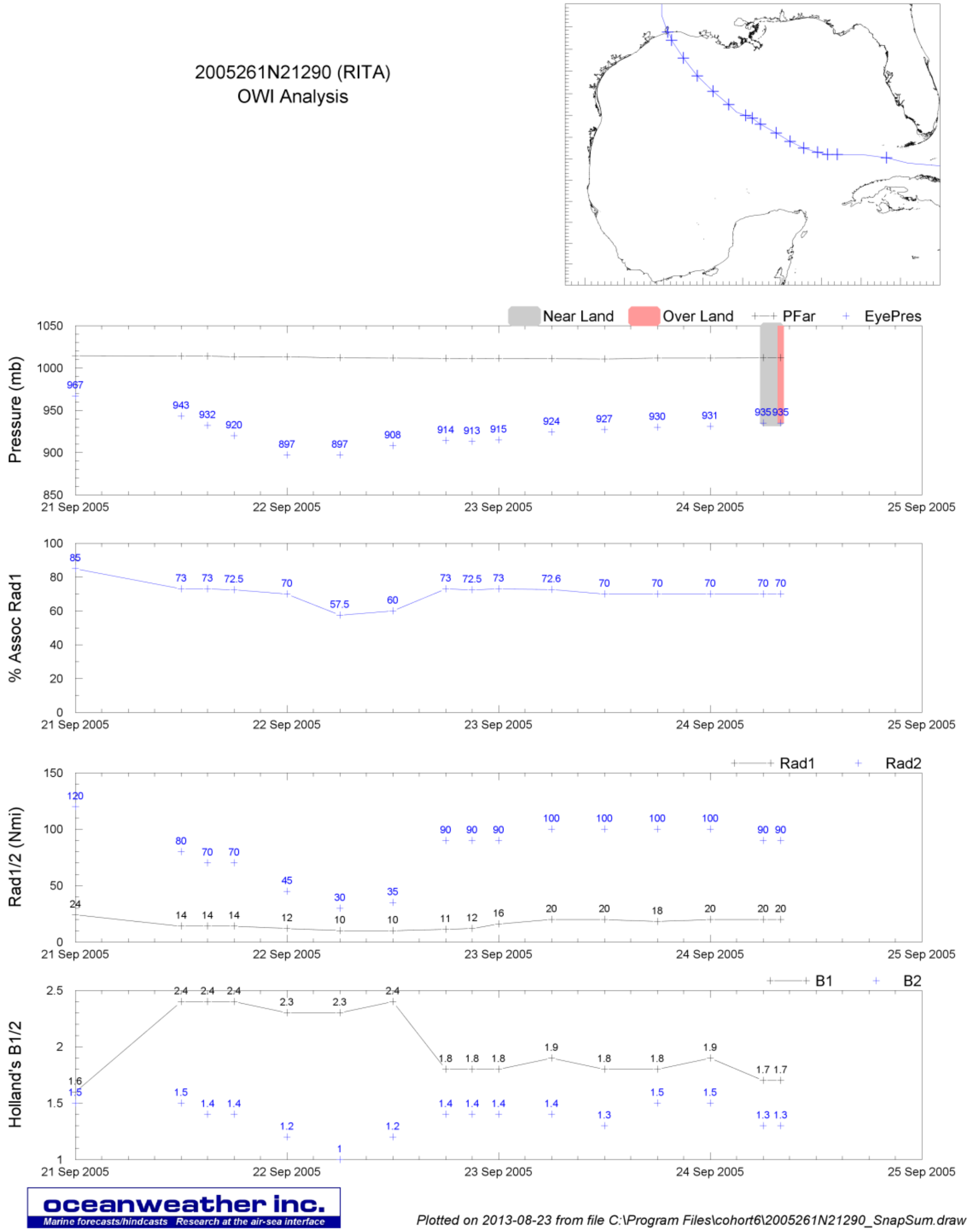


**Figure 6. Summary of model input parameters applied in Rita (2005)**

**0 = No Data**

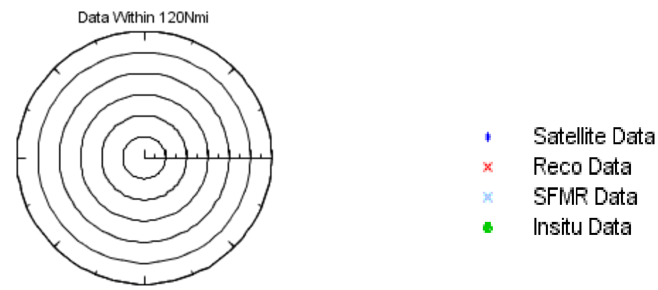


**1 = Insitu/Satellite Only, Incomplete Coverage**

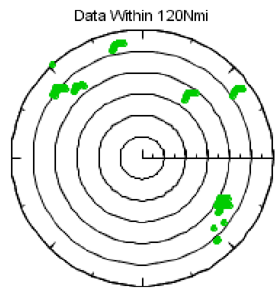


**2 = Insitu/Satellite Only, Coverage in All Quadrants**

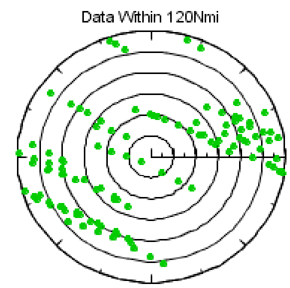


**3 = Sparse Reco, Incomplete Coverage**

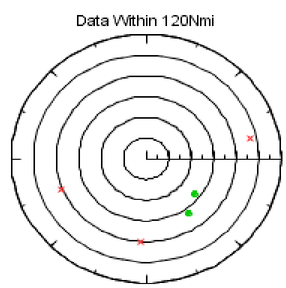


**4 = Sparse Reco, Coverage in All Quadrants**

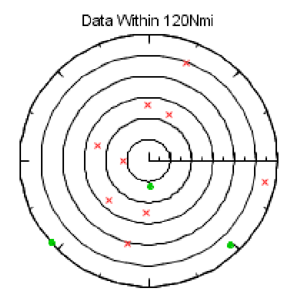


**5 = Hi-Res Reco/SFMR, Incomplete Coverage**

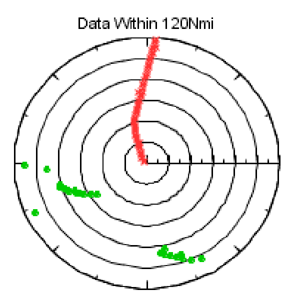


**6 = Hi-Res Reco/SFMR, Coverage in All Quadrants**

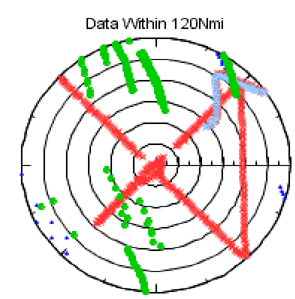


**Figure 7. Data classification key applied in the assessment of data for each snapshot**

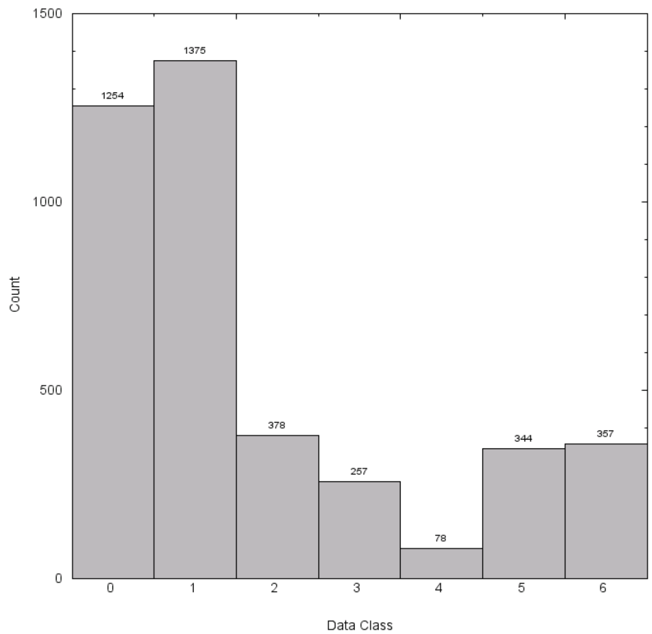


**Figure 8. Distribution of GOMOS snapshots (1900-2011) by data class**

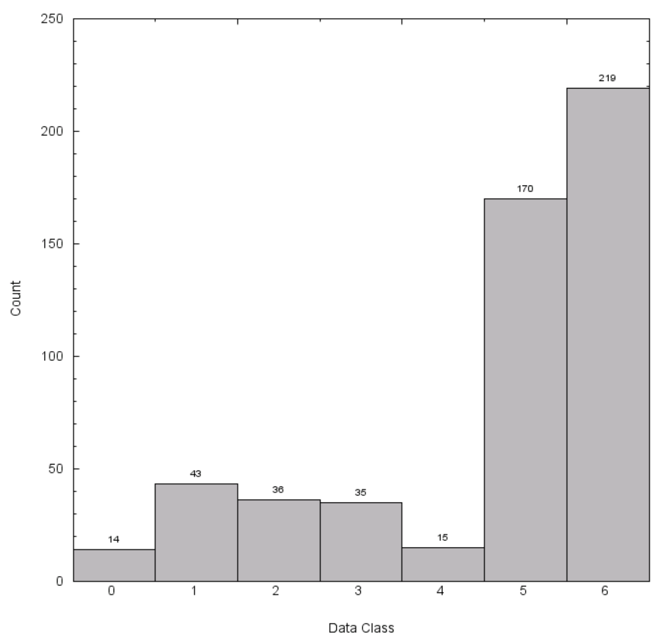


**Figure 9. Distribution of GOMOS snapshots (1900-2011) by data class for fits which applied a double exponential**

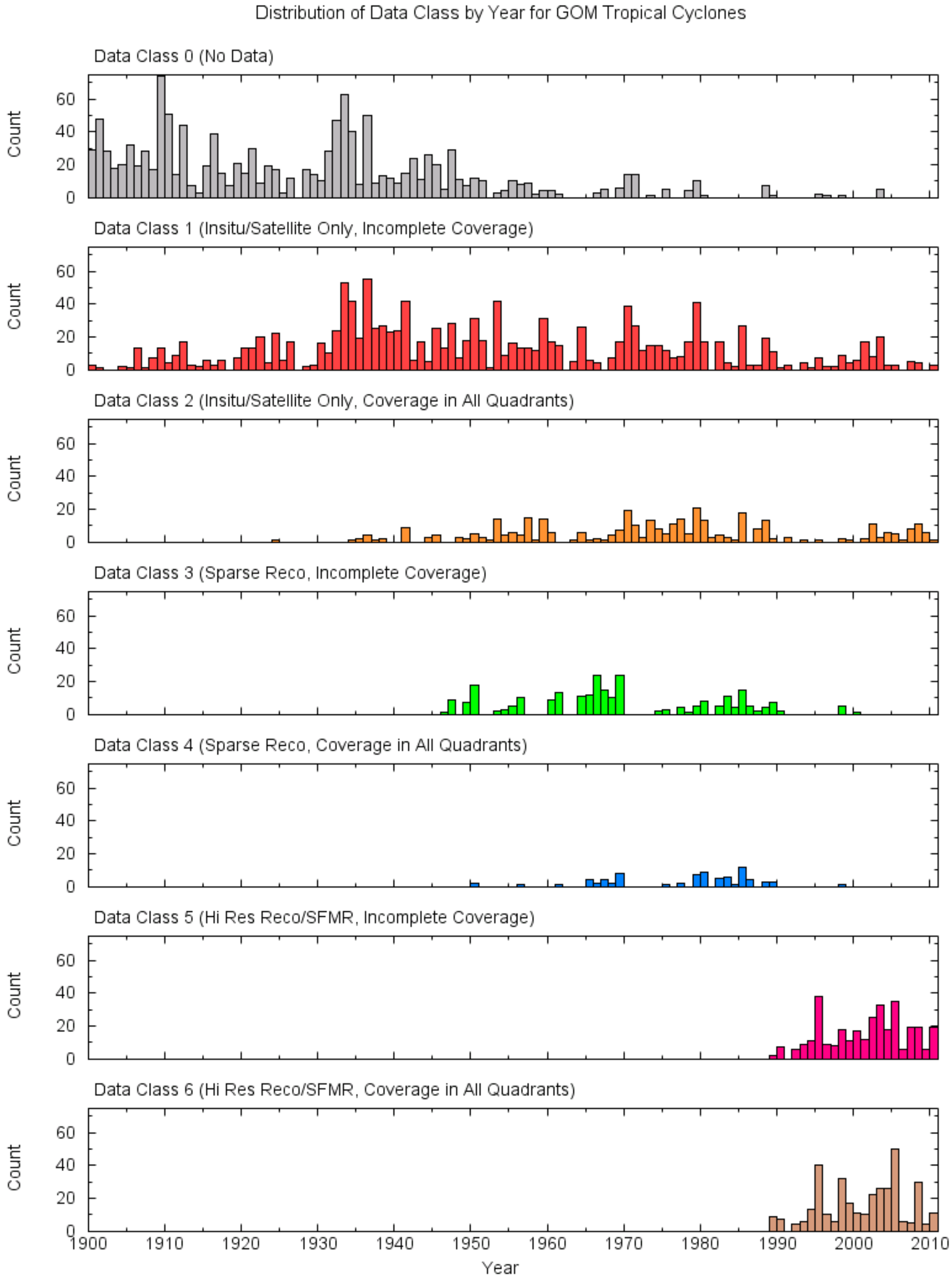


**Figure 10. Data classification by year**

### 2.4 Conceptual Classification Based on Fits to the Radial Wind Profile

Following Chen (2010) et al. we introduce a simple “shelfiness” parameter as follows:

$$S_{GOM} = \frac{Vt_{4RMW}}{Vt_{RMW}} \; x \; \sqrt{\frac{\Delta p}{\Delta p_{ave}}}$$

where $Vt_{4RMW}$ is the wind speed at four times RMW, $\Delta p$ is the total storm pressure anomaly at the snapshot time, $Vt_{RMW}$ is the maximum wind speed at RMW and $\Delta p_{ave}$ is the average total storm pressure anomaly for the average of all GOMOS storms (again like Chen et al. for Po < 990 to eliminate weak tropical storms and depressions). This value, $\Delta p_{ave}$, is 44.72 mb and 45 mb is taken as the average.

A value of $S_{GOM}$ ~ 0.6 appears to delineate more ($S_{GOM}$ > 0.6) or less ($S_{GOM}$ <= 0.6) shelfiness based on a manual inspection of select GOM tropical systems. When applied to the GOMOS parameter fits, a total of 811 (56%) snapshots are below (less shelfiness) the 0.6 threshold and 639 (44%) are above (more shelfiness) based on the full 1900-2011 period (Figure 11). The distribution of $S_{GOM}$ during aircraft reconnaissance period (1947-2011), shows a slightly more even split of 52% below 0.6 and 48% above. All shelf index’s above 0.9 were from the 1947-2011 period suggesting that the more extreme shelfiness cases require aircraft data to properly diagnose a shelf-like structure.

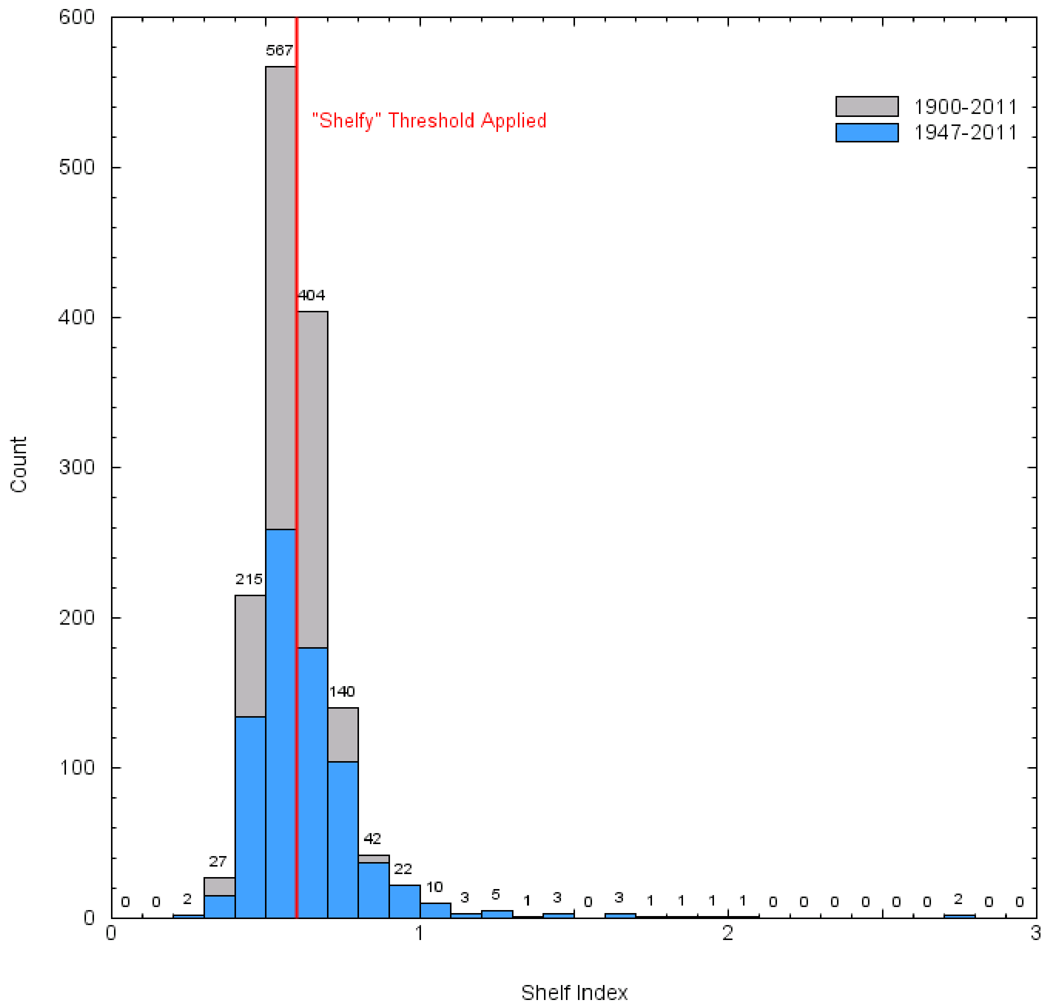


**Figure 11. Distribution of shelf index for GOM tropical snapshots from 1900-2011 and 1947-2011**

Based on examination of many tropical profile fits and clusters of fitting parameters and resulting radial surface wind distribution, the following classes detailed in Table 1 were defined for further study.

**Table 1 Wind profile classification system with typical criteria for $S_{GOM}$, Radius and Holland's B.**

| Class | Description | $S_{GOM}$ | Radius Criteria | B Criteria |
|---|---|---|---|---|
| 1 CSPN | Compact Single Peaked Negligible Shelfiness | ≤0.6 | RMW<24 | B1 > 1 |
| 2 CSPS | Compact Single Peaked Shelfy Outer Core | >0.6 | RMW<24 | - |
| 3 BSPN | Broad Single Peaked Negligible Shelfiness | ≤0.6 | RMW≥24 | - |
| 4 BSPS | Broad Single Peaked Shelfy Outer Core | >0.6 | RMW≥24 | - |
| 5 MPID | Multi Peaked – Inner Dominant | RMW_In_Ws ≥ RMW_Out_Ws | | |
| 6 MPOD | Multi Peaked – Outer Dominant | RMW_In_Ws < RMW_Out_Ws | | |
| 7 SDNP | Shelf Dominant No Peaks | Flat Profile – Manually Determined | | |

### 2.4.1 CSPN: Compact Single Peaked Negligible Shelf

This class conforms most closely to Colon's "Daisy" type and Samsury and Rappaport's "Narrow" type and is, of course, encompassed by Chen et al.'s "Compact" class. Since the mean RMW of all GOMOS snapshots (with Po less than 990 mb) is 23.68 Nm, then RMW < 24 Nm is a convenient marker for this class, which on average corresponds to an Rad1 or about 20 Nm but only in the case of a single exponential fit. Where two exponentials are fitted the RMW will be determined by the relative Rad1/2 and percentage of the total pressure drop carried by the inner exponential. Since even compact single peaked classes can have an energetic outer core, additional discriminants are needed. B1 is a logical case and for this class should be at least 1.0. This class will typically be fitted with a single exponential, however double exponentials do occur but with less than average shelfiness.

A good example of this class is Hurricane Celia (1970) through much of its passage across the northern GOM between August 1-3. Rad1 varied from 10 Nm to 15 Nm, B was generally greater than 1.3 and $S_{GOM}$ tended to be less than 0.5.

### 2.4.2 CSPS: Compact Single Peaked Shelfy Outer Core

For the CSPS class, RMW is again less than 24 Nm, but B1 may be less than 1 and often a second exponential is fitted. Hurricane Dennis (2005) depicts a typical CSPS profile on July 10 0600 UTC with basically no change in flight level or surface wind speed between 30 Nm and 120 Nm of the center. There is a compact inner core with RWM of only ~ 8 Nm. Dennis entered the GOM by crossing central Cuba during which passage its intensity decayed rapidly from Category 4 to Category 1. The passage totally destroyed its inner core leaving a pure shelf-like radial wind profile but it was able to rapidly intensify and regain its inner core over the following 24-hours. Most compact hurricanes that follow this track do not redevelop a tight inner core but environmental conditions for intensification appeared to be especially conducive for development as Dennis entered the GOM.

### 2.4.3 BSPN: Broad Single Peaked Negligible Shelfiness

This class may be fitted by a single or double exponential profile but the inner Rad 1will tend to dominate the fit. A good example of a broad single peaked snapshot with little shelfiness is Hurricane Georges (1998). Georges managed to skirt the north coast of Cuba and enter GOM though the Florida Straits. A double exponential was fitted, but B1 was large at 1.6 and the inner exponential carried 72.5% of the total pressure drop.

### 2.4.4 BSPS: Broad Single Peaked Shelfy Outer Core

As noted above for the compact class, Rad1 may not be a good indicator of RMW. For example, as Katrina (2005) approached the MS Delta, its inner core circulation broadened rapidly and it developed a broad circulation overall. Just before landfall at August 19, 1200 UTC even though its Rad1 is 22 Nm, its RMW is ~ 30 Nm because the second exponential, with Rad1 of 40 Nm, carries as much weight as the inner (pressure drop 50%). B1 is 0.8 and B2 is 1.3.

### 2.4.5 MPID: Multi Peaked – Inner Dominant

This class is always fitted with a double exponential form, but the combinations of variables are so varied that simple discriminant parameter ranges are difficult to define. Fortunately, this class, and its neighbor MPOD, are obvious by simple inspection of the radial profile and, in fact, when a storm is undergoing a single or repetitive eyewall replacement cycle it will transition from one to the other. However, it appears that in the GOM, hurricanes rarely undergo multiple eye-wall replacement cycles. A good example of this class is the previously referenced profile in Hurricane Allen (1980) on August 9 at 0600 UTC. This hurricane is rather distinct for having maintained basically this structure throughout its three-day trek from the Yucatan Strait to the lower Texas Coast including passage through Category 5 intensity early on August 8.

### 2.4.6 MPOD: Multi Peaked – Outer Dominant

Hurricane Ike (2008) on September 11, 0000 UTC is a good example of a MPOD profile with a dominant outer peak. Ike maintained this structure basically from the time the center emerged into the GOM after traversing western Cuba early on September 10 to early on September 12, when the inner peak was completely eroded and the vortex was better characterized as BSPS.

### 2.4.7 SDNP: Shelf Dominant No Peak

This class is characterized by the absence of a distinct peak, which may be defined as the absence of a relative peak of at least 5 knots of magnitude above the background profile. This class is usually a transient state of relatively short duration, but some GOM storms have exhibited longer durations. The best example of SDNP in a well-documented storm is Hurricane Isaac (2012) on August 27/28. During this period, the radial distribution of wind speed was essentially flat from ~ 20 Nm to 120 Nm from the center. Isaac attained peak intensity only of Category 1 within the GOM but the shelf structure induced ocean responses in terms of coastal storm surge and wave heights offshore, which are more typically raised by a major hurricane (Category 3 or greater). Impacts on offshore infrastructure, operations and coastal damage, and loss of life were also much greater than expected of a Category 1 storm.

### 2.5 Distribution of Classes

A team of meteorologists examined each of the profiles in the database and assigned a class to each in a man-machine mix procedure that referred to recommended fitting parameter ranges, the “shelfiness index”, and visual examination.

#### 2.5.1 Overall

In all, 1,450 of 4,043 (36%) GOMOS snapshot fits from 1900-2011 attained a central pressure threshold of 990 mb and were classified using the methodology detailed in Section 2.4. The overall distribution of classes is shown in Figure 12 for both the full 1900-2011 period as well as the aircraft reconnaissance period of 1947-2011. Like the analysis of $S_{GOM}$ shown in Figure 11, the profile classes with the highest $S_{GOM}$ index (dual radius of maximum wind profile classes 5 and 6) are only found in the later (1947-2011) time period. Means of the basic profile parameters of Po, Rad1, Rad2, B1, B2, Dp% and PFar are given for each class in Table 2 and are stratified by single and double exponential pressure profile fits. Most class 1 CSPN profiles apply the single exponential profile (90% of the time) while its shelfy counterpart, class 2 CSPS, 73% of the profiles applied the single exponential fit. The average central pressure for CSPN is 980/977 mb (single/double) while the CSPS fits are on average much stronger at 954/945 mb suggesting that stronger systems exhibit a more shelfly structure. A similar relationship is shown for class 3 BSPN and class 4 BSPS: the shelfier BSPS has a higher percentage of double vs. single exponential fits than BSPN (92% BSPN, 78% BSPS) and are associated with stronger (979/972 mb BSPN, 956/955 mb BSPS) storms. The two classes which exhibit dual wind maxima, class 5 MPID and class 6 MPOD, always apply a double exponential fit. The inner Rad1 for MPID (inner RMW dominate) is on average tighter than MPOD (outer RMW dominate), 11 vs. 15 Nm, and is on average stronger with central pressure of 946 mb vs. 968 mb for MPOD. The flat profile exhibited by class 7 SDNP applies single and double fits nearly equally (10 single vs. 12 doubles) and Rad1 values for singles and Rad2 for double fits are on average the highest of any class (144 and 100 Nm respectively).

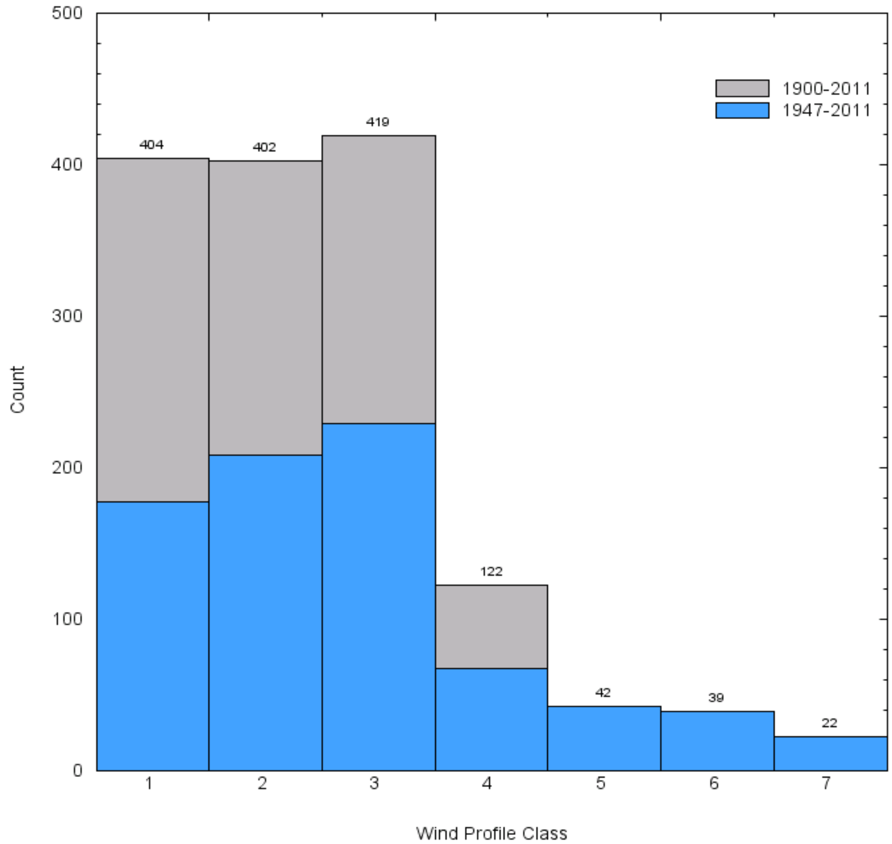


**Figure 12. Distribution of wind profile classes for 1900-2011 and 1947-2011 GOM tropical radial wind snapshots**

**Table 2. Average tropical fit parameters by profile class for single and double exponential fits**

| Profile Class | Exponential Fit | Count | Average EyePres (mb) | Average Rad1 (Nm) | Average Rad2 (Nm) | Average Dp% | Average B1 | Average B2 | Average Pfar | Average Shelf Index |
|---|---|---|---|---|---|---|---|---|---|---|
| 1 (CSPN) | Single | 362 | 980 | 19 | | 100 | 1.10 | | 1013 | 0.54 |
| | Double | 42 | 977 | 16 | 49 | 58 | 1.70 | 1.30 | 1014 | 0.50 |
| 2 (CSPS) | Single | 293 | 954 | 18 | | 100 | 1.20 | | 1012 | 0.68 |
| | Double | 109 | 945 | 16 | 65 | 66 | 1.80 | 1.30 | 1013 | 0.77 |
| 3 (BSPN) | Single | 384 | 979 | 31 | | 100 | 1.20 | | 1013 | 0.50 |
| | Double | 35 | 972 | 32 | 82 | 66 | 1.50 | 1.50 | 1012 | 0.52 |
| 4 (BSPS) | Single | 96 | 956 | 33 | | 100 | 1.20 | | 1013 | 0.71 |
| | Double | 26 | 955 | 31 | 96 | 69 | 1.40 | 1.30 | 1012 | 0.70 |
| 5 (MPID) | Single | 0 | | | | | | | | |
| | Double | 42 | 946 | 11 | 85 | 63 | 1.80 | 1.50 | 1012 | 0.78 |
| 6 (MPOD) | Single | 0 | | | | | | | | |
| | Double | 39 | 968 | 15 | 63 | 50 | 1.10 | 1.80 | 1012 | 0.94 |
| 7 (SDNP) | Single | 10 | 988 | 144 | | 100 | 1.10 | | 1011 | 0.81 |
| | Double | 12 | 981 | 25 | 100 | 53 | 0.70 | 0.70 | 1010 | 0.65 |

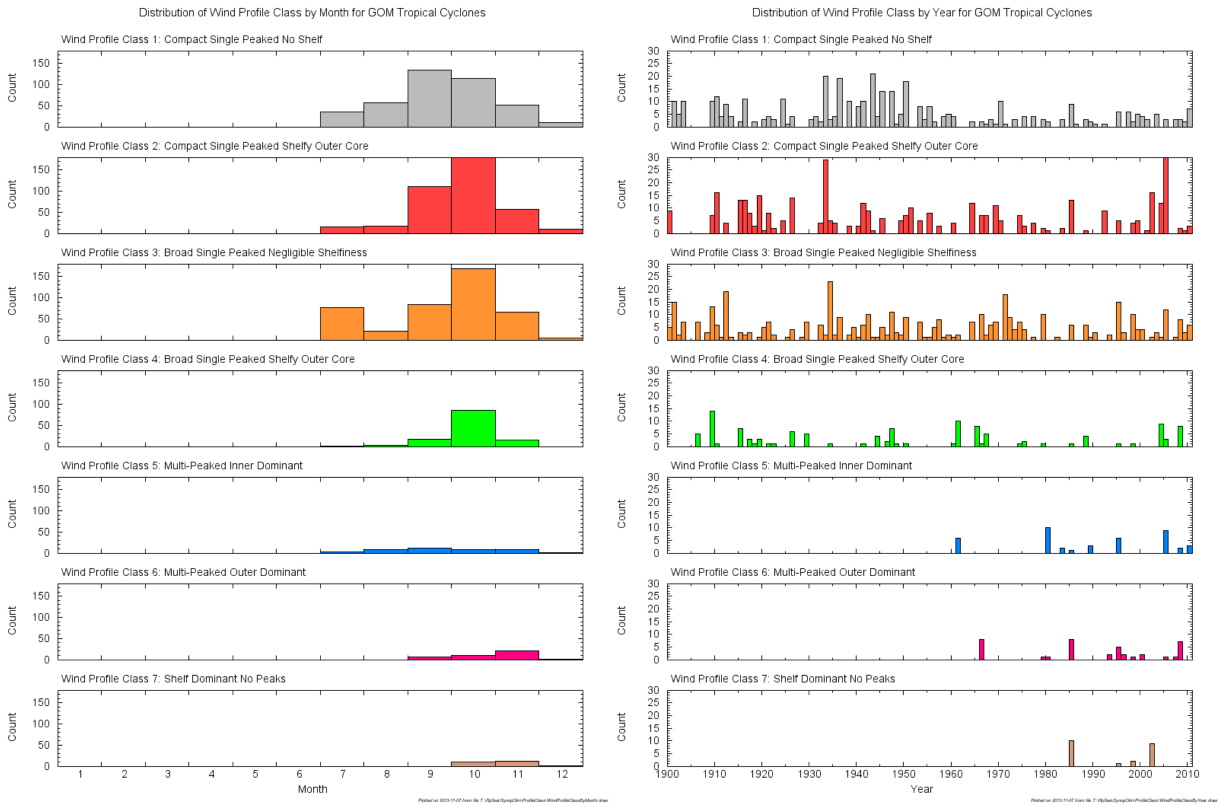


**Figure 13. Monthly (left) and yearly (right) distributions of wind profile classes**

Wind class profiles were stratified by month and year of occurrence as shown in Figure 13. Most of the wind profile classes show a single seasonal peak in either the September or October months. Only the class 3 BDPN profile depicts dual peak months with an early season peak in July and later peak in September. Wind profiles with outer dual maxima (class 6 MPOD) and very broad profiles (class 7 SDNP) both peak later in the season (November) although neither class contain a lot of samples. As shown in the yearly distributions, both these classes (6/7) as well as the dual inner wind class 3 MPID were all fit in the aircraft reconnaissance period 1947-2011. Other profile fits (classes 1-4) are found in nearly all years with little apparent grouping.

### 2.5.2 Classes by Storm Parameter

Profile classes were stratified by central pressure and by forward speed since neither model parameter was applied in the estimation of the profile class, except in the intensity threshold of 990 mb. The central pressure plot (Figure 14, left) confirms the tendency shown in the average Po values by class that the shelfy class 2 CSPS and class 4 BSPS are stronger than their less shelfy class 1 CSPN and class 3 BSPN counterparts. The strongest storms in terms of pressuure appear to be associated with class 2 CSPS and class 5 MPID (inner RMW dominate) storms which both have higher shelf indices. In the forward speed comparisons (Figure 14, right) there appears to be a shift in the peak band with the shelf classes 2/4 translating faster on average than the less shelfy classes 1/3.

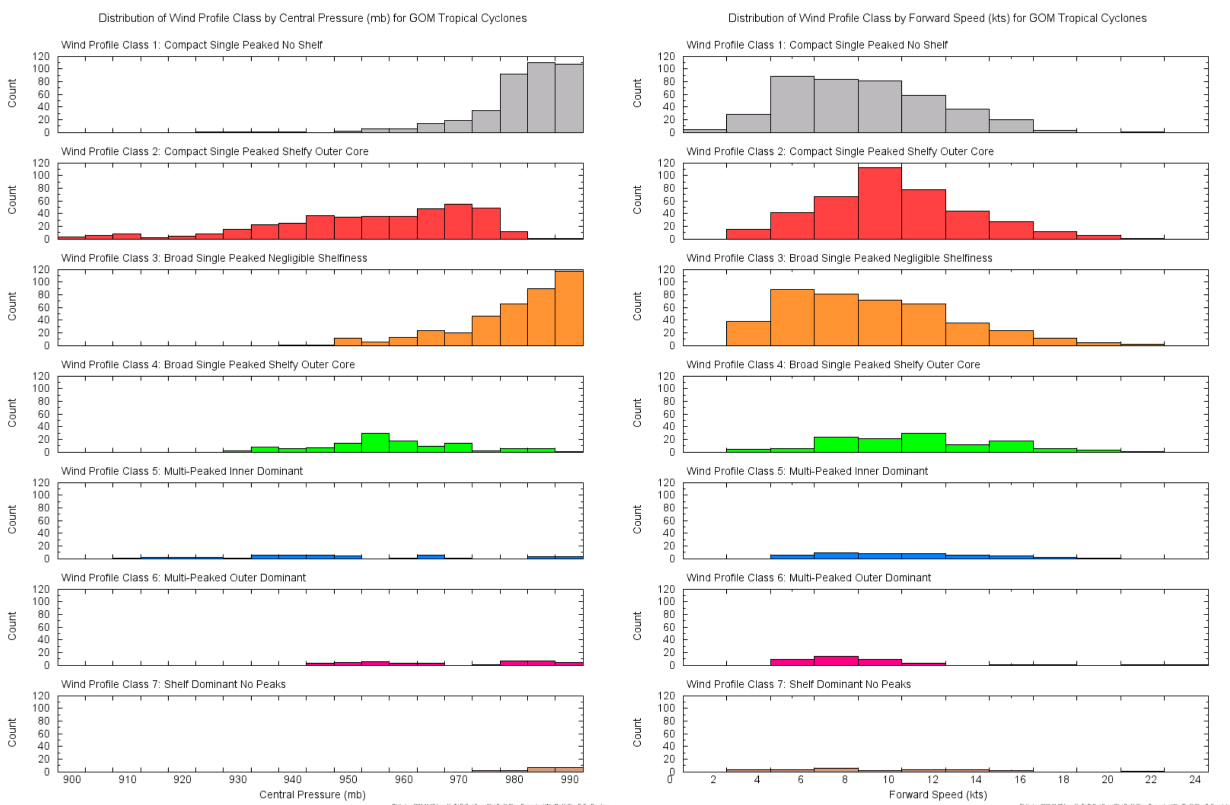


**Figure 14. Distribution of wind profile classes by central pressure (mb, left) and forward speed (kts, right)**

### 2.5.3 Classes by Track Path

When the wind profile classes are plotted by position (Figure 15) there does not appear to be a geographic pattern to the locations of each class. To test if storm history, rather than the instantaneous position, would be a better predictor of wind profile class the storm tracks for the entire population were sorted into six track path classes as shown in Figure 16. Track path Class 0 (TP 0) storms formed in the GOM, Class 1 (TP 1) storms tracked across Florida, Class 2 (TP 2) entered via the Florida Straits, Class 3 (TP 3) crossed Cuba, Class 4 (TP 4) via the Yucatan Straits and finally Class 5 (TP 5) crossed a portion of the Yucatan. No attempt was made to track the storm history previous to the point of entry/origin in the GOM.

The distribution of wind profile classes by track path are summarized in Figure 17. Storms which formed in the GOM (TP 0) had the highest occurrence (77%) of the wind profile classes associated with no shelf (class 1 CSPN) or negligible shelfiness (class 3 BSPN). Track paths with a land influence (TP 1, TP 3, and TP 5) also had a higher percentage of class 1 and 3 profiles at 61%, 53% and 63%, respectively. The two track paths with less land influence via the Florida (TP 2) and Yucatan Straits (TP 4) have the lowest percentage of class 1 and 3 profiles with 19% and 42%, respectively.

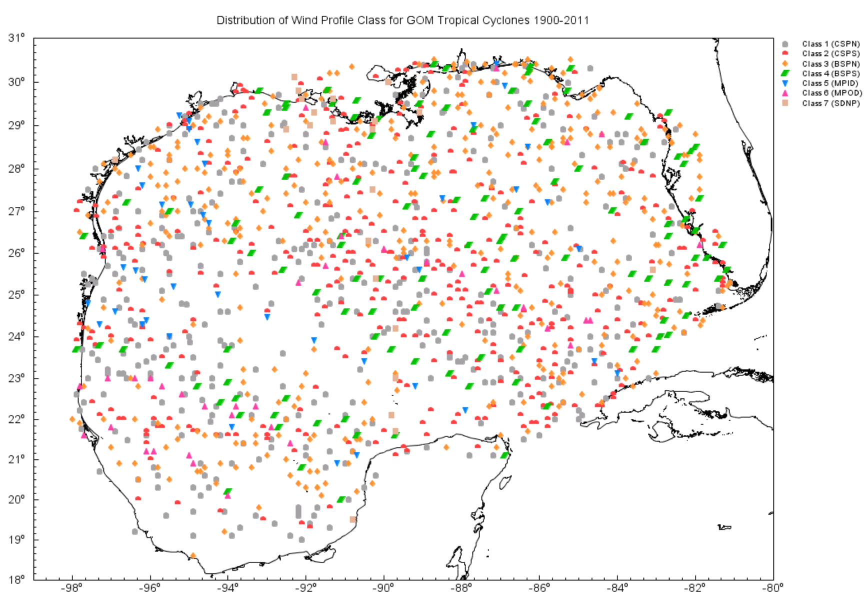


**Figure 15. Location of snapshots color-coded by wind profile class.**

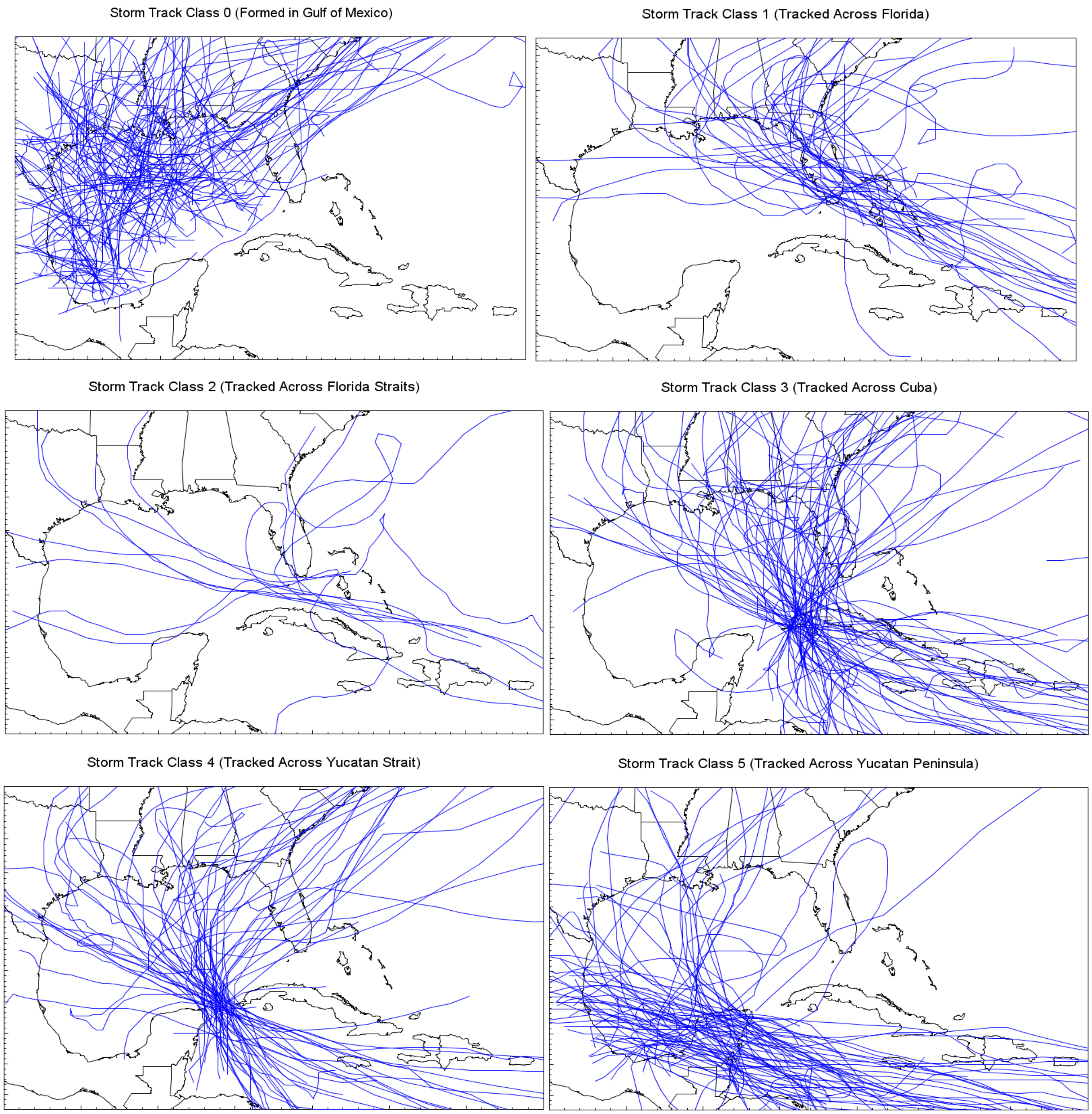


**Figure 16. Track path classes applied for GOM tropical systems**

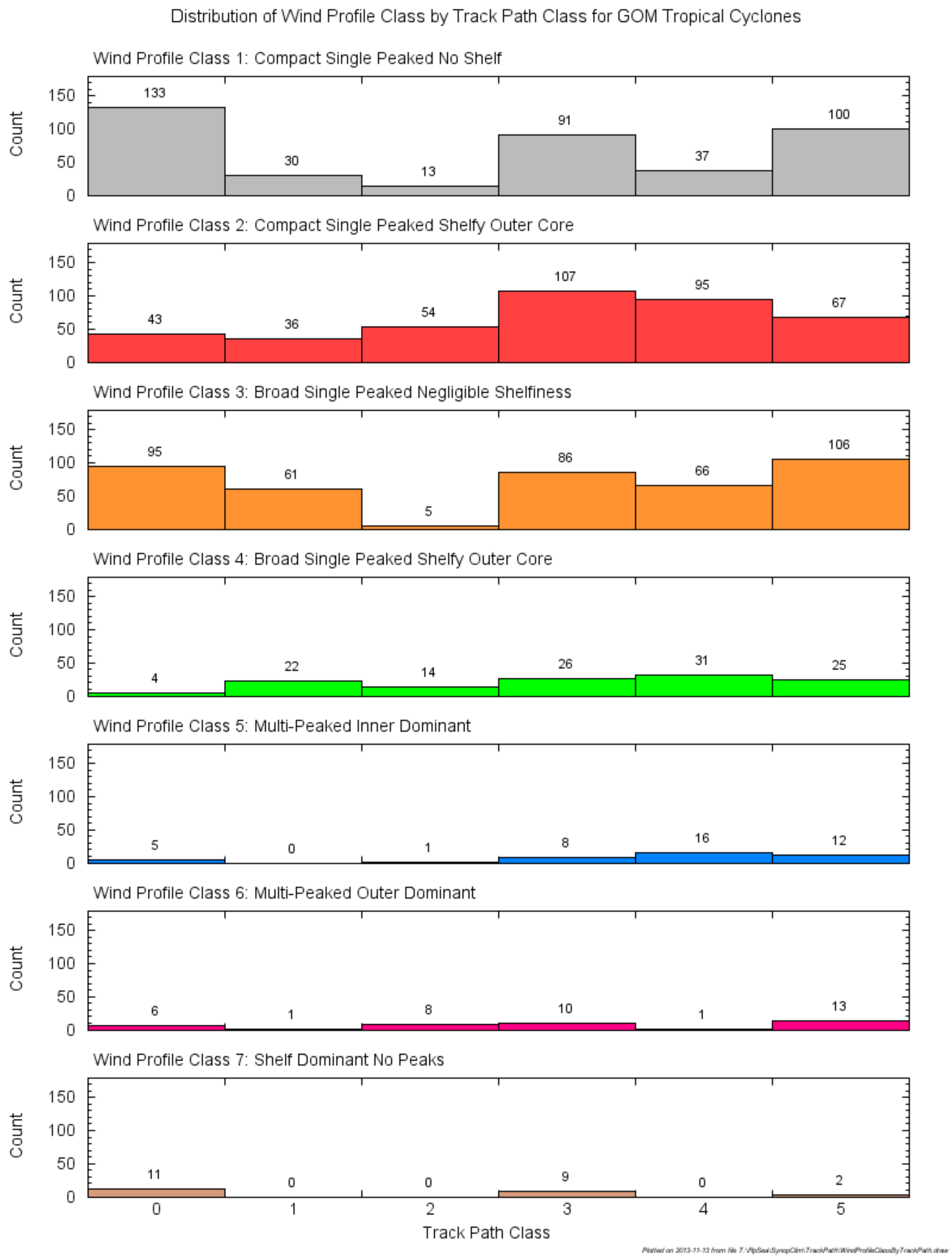


**Figure 17. Distribution of wind profile class by track path**

#### 2.5.4 Characteristic Class Evolution

In the population of wind profile classes found, there are 200 individual storms with at least two adjacent snapshots to investigate how wind profile classes vary during a storm's evolution. Of these 200 storms, 58% (116) storm systems had multiple wind profile classes (Table 3) with the remaining 42% of storms maintaining the same wind profile class throughout the GOM. The most stable classes are 1 and 3 which maintained the same profile class 17% of the time.

**Table 3. Counts of storms which retained a single wind profile class while in the GOM**

| Class | Number of Storms | % of Population |
|---|---|---|
| 1 | 34 | 17% |
| 2 | 11 | 6% |
| 3 | 34 | 17% |
| 4 | 2 | 1% |
| 5 | 1 | <1% |
| 6 | 1 | <1% |
| 7 | 1 | <1% |
| Multiple Wind Profile Class | 116 | 58% |

Snapshot to snapshot variation in wind profile class changes for all storms with at least two adjacent snapshots are shown in Table 4. The analysis was done for all storm snapshots, as well as those at least twice the Rad1 value from land and for storms over the water to test for land influences on wind profile changes. The results for all three stratifications were very similar, with a storm retaining its wind profile from 69.9% to 85% of the time from snapshot to snapshot. The lone exception was the broad class 7 which had no data when the snapshots were restricted to 2 times the Rad1 value. This is likely due to the broadness of the Rad1's in class 7 coupled with the restrictive geographic domain of the GOM.

The largest class change bin was found in the overall analysis in wind profile class 4 BSPS transitioning to a class 3 BSPN 19.4% of the time (a loss of shelfiness). Class 1 profiles transitioning to class 2 (more shelfiness) occurred 12.1% of the time, class 6 transitioning to class 1 (loss of dual wind maxima) occurred 11.8% of the time and class 5 transitioning to class 6 (dual wind transition from inner dominate to outer dominate) occurred 10.8% of the time. No other transitions bin accounted for more than 9% of the population in overall results.

**Table 4 Evolution of wind profile class changes from adjacent snapshot by profile class for all snapshots. No change in class is highlighted in yellow.**

| Wind Profile Evolution for all GOM Snapshots with at least 2 consecutive positions | | | | | | | | | | | | | | | |
|---|---|---|---|---|---|---|---|---|---|---|---|---|---|---|---|
| | | | | | | | | | | | | | | | |
| | | To Class1 | | To Class2 | | To Class3 | | To Class4 | | To Class5 | | To Class6 | | To Class7 | |
| From Class | Class Count | Count | % | Count | % | Count | % | Count | % | Count | % | Count | % | Count | % |
| 1 | 348 | 275 | 79.0 | 42 | 12.1 | 29 | 8.3 | 1 | 0.3 | 0 | 0.0 | 1 | 0.3 | 0 | 0.0 |
| 2 | 365 | 24 | 6.6 | 303 | 83.0 | 13 | 3.6 | 14 | 3.8 | 8 | 2.2 | 2 | 0.5 | 1 | 0.3 |
| 3 | 342 | 25 | 7.3 | 11 | 3.2 | 279 | 81.6 | 23 | 6.7 | 0 | 0.0 | 4 | 1.2 | 0 | 0.0 |
| 4 | 103 | 0 | 0.0 | 9 | 8.7 | 20 | 19.4 | 72 | 69.9 | 1 | 1.0 | 0 | 0.0 | 1 | 1.0 |
| 5 | 37 | 0 | 0.0 | 3 | 8.1 | 1 | 2.7 | 0 | 0.0 | 29 | 78.4 | 4 | 10.8 | 0 | 0.0 |
| 6 | 34 | 4 | 11.8 | 0 | 0.0 | 3 | 8.8 | 2 | 5.9 | 0 | 0.0 | 25 | 73.5 | 0 | 0.0 |
| 7 | 20 | 0 | 0.0 | 0 | 0.0 | 1 | 5.0 | 0 | 0.0 | 1 | 5.0 | 1 | 5.0 | 17 | 85.0 |
| | | | | | | | | | | | | | | | |

## 3. SUMMARY AND CONCLUSIONS

This paper describes the development and analysis of a classification system for the radial wind profile in Gulf of Mexico tropical systems. This work was part of a larger Research Partnership to Secure Energy for America (RpSea) project (10121-4801-01) to develop an Ultra-Deepwater Synthetic Hurricane Risk Model for the Gulf of Mexico. Tropical fits and analysis described in this paper will be applied and validated within the risk model.

It was found that nearly one half of GOM tropical cyclones (48% for 1947-2011) depict a shelf like structure to the radial wind profile based on the $S_{GOM}$ index described in this paper. Most storms depict a single radius of maximum winds, while dual radius of maximum wind (Classes 5 and 6) make up just 5.6% of the storm population. All dual radius of maximum wind storms were analyzed during the aircraft reconnaissance period of post 1947.

Storms which form within the GOM have the highest occurrence (77%) of wind profile classes with negligible shelfiness ($S_{GOM}$ <0.6, Classes 1 and 3) in the radial wind profile. Class 1/3 storms were also most likely to retain a single profile class over the storm lifetime in the GOM. On average, 58% of the storms exhibited multiple wind profile classes during their GOM lifetime. Storms kept the same wind profile class 70-85% of the time in adjacent six-hourly fits.

Strongest storms, on average, were typically analyzed with a double exponential pressure profile fits in Class 2 (compact with shelf) or Class 5 (multiple peak, inner dominant).

This paper is dedicated to the memory of Vincent J. Cardone (1941-2013) who greatly contributed to the project reported here. His lifetime contribution of work in marine meteorology, air/sea interaction and wave modeling has left a lasting legacy for the entire metocean community. He is greatly missed.

**References**

Cardone, V.J., and A.T. Cox, 2009. Tropical cyclone wind field forcing for surge models: critical issues and sensitivities. Natural Hazards: Volume 51, Issue 1 (2009), Page 29.

Chen, Y.C., K.K.W. Cheung nd C. Lee, 2010. Some Implications of Core Regime Wind Structures in Western North Pacific Tropical Cyclones. Wea. And Fore., Vol 26, No 1, Feb 2011.

Colon, J.A. 1963. On the evolution of the wind field during the life cycle of tropical cyclones. National Hurricane Research Project Report 65.

Merrill, Robert T., 1984: A Comparison of Large and Small Tropical Cyclones. Monthly Weather Review Volume 112, Issue 7, pp. 1408-1418.

Samsury, C. E., and E. N. Rappaport, 1991: Predicting Atlantic hurricane intensity from research and reconnaissance aircraft data. Preprints, 19th Conf. on Hurricanes and Tropical Meteorology, Miami, FL, Amer. Meteor. Soc., 516–520.

Shen, W. 2006. Does the size of hurricane eye matter with its intensity? Geo. Res. Let. Vol 33, 2006.